

Nambu-Goldstone dark matter and cosmic ray electron and positron excess

This article has been downloaded from IOPscience. Please scroll down to see the full text article.

JHEP04(2009)087

(<http://iopscience.iop.org/1126-6708/2009/04/087>)

[The Table of Contents](#) and [more related content](#) is available

Download details:

IP Address: 80.92.225.132

The article was downloaded on 03/04/2010 at 10:32

Please note that [terms and conditions apply](#).

Nambu-Goldstone dark matter and cosmic ray electron and positron excess

Masahiro Ibe,^a Yu Nakayama,^{b,c} Hitoshi Murayama^{b,c,d} and Tsutomu T. Yanagida^{d,e}

^a*SLAC National Accelerator Laboratory,
Menlo Park, CA 94025, U.S.A.*

^b*Department of Physics, University of California,
Berkeley, CA 94720, U.S.A.*

^c*Theoretical Physics Group, LBNL,
Berkeley, CA 94720, U.S.A.*

^d*Institute for the Physics and Mathematics of the Universe, University of Tokyo,
Kashiwa 277-8568, Japan*

^e*Department of Physics, University of Tokyo,
Tokyo 113-0033, Japan*

E-mail: ibe@slac.stanford.edu, nakayama@berkeley.edu,
hitoshi.murayama@ipmu.jp, tsutomu.ty@hep-th.phys.s.u-tokyo.ac.jp

ABSTRACT: We propose a model of dark matter identified with a pseudo-Nambu-Goldstone boson in the dynamical supersymmetry breaking sector in a gauge mediation scenario. The dark matter particles annihilate via a below-threshold narrow resonance into a pair of R-axions each of which subsequently decays into a pair of light leptons. The Breit-Wigner enhancement explains the excess electron and positron fluxes reported in the recent cosmic ray experiments PAMELA, ATIC and PPB-BETS without postulating an overdensity in halo, and the limit on anti-proton flux from PAMELA is naturally evaded.

KEYWORDS: Cosmology of Theories beyond the SM, Supersymmetric Standard Model

ARXIV EPRINT: [0902.2914](https://arxiv.org/abs/0902.2914)

Contents

1	Introduction	1
2	General discussion on the hidden sector dark matter	2
3	Nambu-Goldstone dark matter	4
3.1	Vector-like SUSY breaking model	4
3.2	Dark matter without R-symmetry breaking	5
3.2.1	R-symmetric spectrum of the light particles	5
3.2.2	Dark matter annihilation without resonance	6
3.3	Nambu-Goldstone dark matter with R-symmetry breaking	7
3.3.1	R-symmetry breaking	7
3.3.2	Spectrum and interactions of light particles	8
3.3.3	Flaton decay	9
3.3.4	Dark matter annihilation via the s -channel flaton	10
3.3.5	Dark matter density and Breit-Wigner enhancement	11
3.3.6	R-axion decay and anti-proton flux	13
4	Conclusion	14
A	Coleman-Weinberg potential of IYIT model	14
B	R-breaking in gauged IYIT model	16
C	F-flaton decay into the SSM particle	17

1 Introduction

Existence of non-baryonic dark matter as the dominant component of matter in the universe has been established by numerous observations. The origin of the dark matter, however, has not been identified yet, and its nature is arguably the most important problem in particle and astrophysics.

Recent observations of ATIC [1] and PPB-BETS [2] balloon experiments show the existence of a bump in a 300-800 GeV energy region of $e^- + e^+$ flux in cosmic ray. The interesting astrophysical possibilities for the origin of the excesses are nearby pulsars [3-5] or supernovae remnants [6]. The most exciting interpretation of the excess, however, is the annihilation and/or decay of the dark matter with a mass in a TeV range. It is remarkable that it explains simultaneously the anomalous excess of e^+ flux in PAMELA experiments [7].

From the theoretical point of view, it is very interesting to explain the dark matter in the supersymmetric (SUSY) extension of the standard model (SSM), since the SUSY models naturally possess two types of candidates for the dark matter. One that has been discussed extensively in the literature is the lightest SUSY particle called as the LSP [8], and the other often overlooked is stable composite “baryons” in a dynamical supersymmetry breaking sector [9]. The former case, however, implies that the masses of the gluino and squarks are much larger than a TeV range, which causes serious problems in discoveries of SUSY particles at the LHC. The latter case predicts most likely the mass of the dark matter to be in at least about 30 TeV, and hence, it seems difficult to explain the dark matter with a TeV mass.

In this paper, we propose a model where the dark matter with a TeV mass is nothing but pseudo-Nambu-Goldstone bosons generated by the SUSY breaking sector (as in the latter case above). Surprisingly, this model provides solutions to the two puzzles in the recent cosmic ray experiments. The first puzzle is that the required annihilation cross section in the galactic halo is much larger (by a factor of $O(100)$) than the one appropriate to explain the dark matter relic density precisely measured by the WMAP experiment [10]. The second puzzle is that the PAMELA experiment sees no excess in the anti-proton flux while it sees an excess of the anti-electron flux.

As we will see, in the Nambu-Goldstone dark matter scenario, the observed dark matter abundance is achieved only if the annihilation process occurs near the pole of a narrow resonance. This inevitably evokes the Breit-Wigner enhancement of the dark matter annihilation [11] (see refs. [12, 13] for earlier attempts) which explains the so-called boost factor. Furthermore, we will see that the dominant final state of the near-pole annihilation is a pair of the R-axions each of which subsequently decays into a light lepton pair. Therefore, this model also provides a concrete example of the scenario [14, 15] explaining the second puzzle in the PAMELA data.

The organization of the paper is as follows. In section 2, we will discuss generic features of the dark matter in the SUSY breaking sector in the light of the recent cosmic ray experiments. In section 3, we propose the Nambu-Goldstone dark matter where the dark matter annihilates via a narrow resonance into an R-axion pair. The final section is devoted to our conclusion.

2 General discussion on the hidden sector dark matter

The idea of the dark matter in the SUSY breaking sector in gauge mediation models was first sketched in ref. [9]. When the SUSY breaking sector possesses a global symmetry, the lightest particle which is charged under the global symmetry is stable and can be a candidate of the dark matter. In earlier attempts, the mass of the dark matter was postulated to be of the order of the dynamical SUSY breaking scale, i.e., around 30 TeV, which is the lowest possible scale realized in gauge mediation scenarios [16–19]. However, such a heavy dark matter is not favorable to explain the observed bump in a 300-800 GeV energy region of $e^- + e^+$ flux in cosmic ray [1, 2]. Therefore, in order to obtain a viable

dark matter model in the SUSY breaking sector, we need to consider some mechanisms to realize a “light” dark matter candidates in the hidden sector.

The simplest possibility to obtain such a light particle is to introduce a small coupling so that the dark matter candidates have a small mass, i.e.,

$$m_{\text{DM}} = \varepsilon \Lambda_{\text{SUSY}}, \tag{2.1}$$

where m_{DM} is the mass of the dark matter which is suppressed by a small coupling ε compared with the SUSY breaking scale Λ_{SUSY} . The dark matter with mass in a TeV range requires

$$\varepsilon = 10^{-(1-2)}, \tag{2.2}$$

when the SUSY breaking scale is around 30 TeV. However, the introduction of the small coupling naively ends up with a too small annihilation cross section to explain the observed dark matter abundance. That is, the naive estimation of the annihilation cross section of the dark matter at the freeze-out time,

$$\begin{aligned} \sigma v_{\text{rel}} &\sim \frac{\varepsilon^4}{16\pi} \frac{1}{m_{\text{DM}}^2} \sim \frac{1}{16\pi} \left(\frac{m_{\text{DM}}}{\Lambda_{\text{SUSY}}} \right)^4 \frac{1}{m_{\text{DM}}^2}, \\ &\sim 10^{-14} \text{ GeV}^{-2} \times \left(\frac{m_{\text{DM}}}{1 \text{ TeV}} \right)^2 \left(\frac{30 \text{ TeV}}{\Lambda_{\text{SUSY}}} \right)^4, \end{aligned} \tag{2.3}$$

is too small to explain the observed dark matter abundance which requires,

$$\sigma v_{\text{rel}} \sim 10^{-9} \text{ GeV}^{-2}. \tag{2.4}$$

Here, we are assuming that the final state is lighter particles in the hidden sector which eventually decay into the SSM particles. Besides, since we are assuming the models with gauge mediation, the coupling between the hidden sector and the SSM sector is rather suppressed (see also discussion in section 3).

A more ambitious possibility is to identify the light dark matter to the pseudo-Nambu-Goldstone bosons resulting from a spontaneous breaking of an approximate global symmetry in the SUSY breaking sector in analogy with the pions in QCD. In this case, we do not need to introduce small couplings to realize the light dark matter. However, the naive estimation of the annihilation cross section of the dark matter is again suppressed, i.e.,

$$\sigma v_{\text{rel}} \sim \frac{1}{16\pi} \left(\frac{m_{\text{DM}}}{\Lambda_{\text{SUSY}}} \right)^4 \frac{1}{m_{\text{DM}}^2}, \tag{2.5}$$

where we have assumed the breaking scale of the approximate global symmetry to be of the order of Λ_{SUSY} .

Theses lessons tell us that the annihilation cross section of the dark matter must be enhanced than the above naive expectations. As an interesting possibility, such enhancement can be realized if we assume that the dark matter annihilates via a narrow resonance with mass $M \simeq 2 m_{\text{DM}}$. This observation, in turn, suggests the possible enhancement of the dark matter cross section in the galactic halo by the Breit-Wigner enhancement mechanism [11]. In the following section, we construct a model of the Nambu-Goldstone dark matter where these possibilities are realized.

3 Nambu-Goldstone dark matter

In this section, we construct an explicit model of the Nambu-Goldstone dark matter based on a dynamical SUSY breaking model. For that purpose, we consider a vector-like SUSY breaking model developed in ref. [20]. As we will see, this model possesses all the necessary ingredients to realize the Nambu-Goldstone dark matter model where the Breit-Wigner enhancement explains the effective boost factor and the R-axion final state explains the no excess in anti-proton flux.

3.1 Vector-like SUSY breaking model

The vector-like SUSY breaking model is based on an SU(2) gauge theory with four fundamental representation fields $Q_i (i = 1, \dots, 4)$ and six singlet fields $S_{ij} = -S_{ji} (i, j = 1, \dots, 4)$ [20]. In this model, the SUSY is dynamically broken when the Q 's and S 's couple in the superpotential,

$$W = \lambda_{ij} S_{ij} Q_i Q_j, \quad (i < j), \tag{3.1}$$

where λ_{ij} denotes coupling constants. The maximal global symmetry this model may have is $SP(4) \simeq SO(6)$ symmetry which requires $\lambda_{ij} = \lambda$. The SUSY is broken as a result of the tension between the F -term conditions of S 's and Q 's. That is, the F -term conditions of S_{ij} , $\partial W / \partial S_{ij} = \lambda_{ij} Q_i Q_j = 0$, contradict with the quantum modified constraint $\text{Pf}(M_{ij}) = \Lambda_{\text{dyn}}^2$ where M_{ij} denote composite gauge singlets made from $Q_i Q_j$. Especially, when the coupling constants λ_{ij} are smaller than unity, the SUSY is mainly broken by the F -term of a linear combination of the singlets S_{ij} .

The effective theory below the dynamical scale Λ_{dyn} is well-described by the gauge singlets M_{ij} and S_{ij} with the effective superpotential,

$$\begin{aligned} W_{\text{eff}} &= \lambda_{ij} \Lambda_{\text{dyn}} S_{ij} M_{ij} + X (\text{Pf}(M) - \Lambda_{\text{dyn}}^2), \quad (i < j), \\ &= \sum_{A=0-5} \lambda_A \Lambda_{\text{dyn}} S_A M_A + X \left(\sum_{A=0-5} M_A^2 - \Lambda_{\text{dyn}}^2 \right), \end{aligned} \tag{3.2}$$

where X is a Lagrange multiplier field which enforces the quantum modified constraint, and we have rearranged the S_{ij} and M_{ij} by using appropriate linear combinations in the last expression. Here, we have assumed that the effective composite operators M_A are canonically normalized (up to order one ambiguity in the coefficient that we will neglect in the following).¹

Now let us assume that the SUSY breaking sector possesses an $SO(5) \subset SO(6)$ global symmetry, and take $\lambda = \lambda_0$ and $\lambda' = \lambda_{a=1-5}$ with $\lambda < \lambda'$. In this case, the lightest particle which is charged under the $SO(5)$ symmetry is stable and can be the dark matter candidate. Under these assumptions, the quantum modified constraint is solved by,

$$M_0 = \sqrt{\Lambda_{\text{dyn}}^2 - \sum_{a=1-5} M_a^2}. \tag{3.3}$$

¹If we use the naive dimensional analysis [21], Λ_{dyn} is replaced with $\Lambda_{\text{dyn}}/4\pi$ without affecting the following discussions.

By plugging M_0 into the effective superpotential in eq. (3.2), we obtain

$$W_{\text{eff}} \simeq \lambda \Lambda_{\text{dyn}}^2 S_0 - \sum_{a=1-5} \frac{\lambda}{2} S_0 M_a^2 + \sum_{a=1-5} \lambda' \Lambda_{\text{dyn}} S_a M_a + O(M_a^4). \quad (3.4)$$

Thus, in terms of the low energy effective theory, the SUSY breaking vacuum is given by,

$$F_{S_0} = \lambda \Lambda_{\text{dyn}}^2, \quad S_a = 0, \quad M_a = 0. \quad (3.5)$$

3.2 Dark matter without R-symmetry breaking

3.2.1 R-symmetric spectrum of the light particles

Before introducing the R-symmetry breaking, it is worth considering the model with no R-symmetry breaking, i.e., $\langle S_0 \rangle = 0$, which clarifies the necessity of the R-symmetry breaking. In the case of the R-symmetric vacuum, the mass spectrum is given as follows. First, the lightest particle which is charged under the SO(5) comes from the scalar components of M_a whose masses squared are given by,

$$m_{\pm}^2 = (\lambda'^2 \pm \lambda^2) \Lambda_{\text{dyn}}^2, \quad (3.6)$$

where the minus sign corresponds to the real component of the M_a scalar. The λ dependence comes from the SUSY breaking effect coming through the $S_0 M_a^2$ coupling in eq. (3.4). On the other hand, the scalar part S_a does not receive the SUSY breaking effects, and has the same mass with the fermion components of S_a and M_a , i.e.,

$$m_{S_a} = m_{M_a} = \lambda' \Lambda_{\text{dyn}}. \quad (3.7)$$

Therefore, we find that the dark matter is given by $\text{Re}[M_a]$.

The masses of the S_0 components require attention. Since the scalar component corresponds to a classical flat direction, its mass vanishes at the tree-level. The one-loop Coleman-Weinberg potential of S_0 , however, gives rise to the mass of S_0 as (see appendix A),

$$m_{S_0} \sim \frac{\lambda^3}{(4\pi)\lambda'} \Lambda_{\text{dyn}}. \quad (3.8)$$

In contrast, the fermion component of S_0 contains the goldstino which acquires a very small gravitino mass by coupling to supergravity.

By putting it all together, we find that the masses of the dark matter as well as the other components of S_a , M_a and S_0 are parametrically lighter than the dynamical scale Λ_{dyn} . For example, we obtain a light dark matter for small couplings,

$$m_{\text{DM}} \simeq \varepsilon \Lambda_{\text{SUSY}}, \quad \varepsilon = O(\lambda^{1/2}, \lambda'^{1/2}), \quad (3.9)$$

where we have used $\Lambda_{\text{SUSY}} = \lambda^{1/2} \Lambda_{\text{dyn}}$ and $\lambda \lesssim \lambda'$. Thus, the dark matter with a mass in a TeV range can be achieved for

$$\varepsilon = 10^{-(1-2)}, \quad (\lambda, \lambda' = 10^{-(2-4)}). \quad (3.10)$$

The above spectrum also poses the other possibility discussed in the previous section, i.e., the pseudo-Nambu Goldstone boson dark matter. We can see it by taking the limit of $SO(6)$ global symmetry, i.e., $\lambda \rightarrow \lambda'$. There, the mass of the dark matter in eq. (3.6) vanishes. This shows that the dark matter is nothing but the pseudo-Nambu-Goldstone boson of the spontaneous breaking of $SO(6)_{\text{app}} \rightarrow SO(5)$ with a breaking scale Λ_{dyn} (see eq. (3.3)). In this case, we obtain the dark matter with a TeV mass for

$$\lambda' - \lambda = O(10^{-(2-4)}), \tag{3.11}$$

while keeping λ and λ' of the order of one.

3.2.2 Dark matter annihilation without resonance

Now, let us consider the dark matter annihilation. For, $m_{S_0} < m_{\text{DM}}$, the dark matter $\text{Re}[M_a]$ dominantly annihilates into S_0 scalar via the F -term potential $|m_{S_a} S_a - \lambda S_0 M_a|^2$ (see eq. (3.4)). The amplitude of this process is given by,

$$\mathcal{M} = \lambda^2 + \lambda^2 \frac{m_{S_a}^2}{t - m_{S_a}^2} = \lambda^2 \frac{t}{t - m_{S_a}^2}, \tag{3.12}$$

where t denotes the momentum transfer. The first term comes from the four-point interaction and the second term from the t -channel exchange of the S_a scalars. In the S -wave limit, the momentum transfer is given by,

$$t = -m_{\text{DM}}^2 \beta_f^2, \quad \beta_f = \sqrt{1 - \frac{m_{S_0}^2}{m_{\text{DM}}^2}} \simeq 1, \tag{3.13}$$

and the cross section is given by,

$$\begin{aligned} \sigma v_{\text{rel}} &= \frac{\beta_f}{8\pi} \frac{v_{\text{rel}}}{2(2m_{\text{DM}})^2 \beta_i} \lambda^4 \left(\frac{t}{t - m_{S_a}^2} \right)^2, \\ &\simeq \frac{\lambda^4}{32\pi} \frac{\beta_f^5}{m_{\text{DM}}^2} \left(\frac{m_{\text{DM}}^2}{m_{S_a}^2} \right)^2. \end{aligned} \tag{3.14}$$

where the final approximation is valid for $m_{\text{DM}} \lesssim m_{S_a}$.²

From this expression, we confirm that the cross section of the “light” dark matter, i.e. $\lambda, \lambda' = 10^{-(2-4)}$ (eq. (3.10)) or $m_{\text{DM}} \simeq 1 \text{ TeV}$ and $m_{S_a} \simeq 30 \text{ TeV}$ (eq. (3.11)), is highly suppressed. So, we need to look for an appropriate narrow resonance so that the cross section is sufficiently enhanced. Interestingly, in the case of the Nambu-Goldstone dark matter, there is a candidate for such a resonance, the scalar part of S_0 . The eq. (3.8) shows that the mass of S_0 scalar can be also in a TeV range for $\lambda \lesssim 1$, and hence, the S_0 mass can satisfy $m_{S_0} \simeq 2 m_{\text{DM}}$ with a careful tuning. Thus, if the dark matter annihilates via the S_0 resonance, the annihilation cross section can be drastically enhanced from the one given above. However, for this process, the R-symmetry must be broken, since the R-charge of S_0 is 2, while that of M_a is 0. Motivated by these observations, we will extend our analysis to the model with the R-symmetry breaking.

²For $m_{S_0} > m_{\text{DM}}$, the dark matter dominantly annihilates into the gravitinos with a much more suppressed annihilation cross section.

3.3 Nambu-Goldstone dark matter with R-symmetry breaking

3.3.1 R-symmetry breaking

Now, let us consider spontaneous R-symmetry breaking. For simplicity, we assume that the R-symmetry is broken by effects of higher dimensional operators of S_0 in the Kähler potential,

$$K = |S_0|^2 + \frac{|S_0|^4}{4\Lambda_4^2} - \frac{|S_0|^6}{9\Lambda_6^4} + \dots, \quad (3.15)$$

where Λ 's denote the dimensionful parameters and the ellipsis denotes the higher dimensional terms of S_0 . The positivity of the coefficient of the quartic term is crucial to destabilize the R-symmetric vacuum at $S_0 = 0$. Notice that the above Kähler potential provides an effective description of a quite general class of the models with spontaneous breaking of the R-symmetry breaking. Especially, when the above Kähler potential results from radiative corrections from physics at the scale Λ_{dyn} , the dimensionful parameters are expected to be,

$$\frac{1}{\Lambda_4^2} = \frac{c_4^2}{16\pi^2} \frac{1}{\Lambda_{\text{dyn}}^2}, \quad \frac{1}{\Lambda_6^4} = \frac{c_6^2}{16\pi^2} \frac{1}{\Lambda_{\text{dyn}}^4}, \quad (3.16)$$

where dimensionless coefficients $c_{4,6}$ are of the order of unity. In appendix B, we demonstrate an explicit perturbative model which breaks the R-symmetry in a similar way studied in ref. [22].

From the above Kähler potential, the R-symmetry is spontaneously broken by the vacuum expectation value of the scalar component of S_0 ;

$$\langle S_0 \rangle = \frac{1}{\sqrt{2}} \frac{\Lambda_6^2}{\Lambda_4} = \frac{1}{\sqrt{2}} \frac{c_4}{c_6} \Lambda_{\text{dyn}} = \frac{1}{\sqrt{2}} f_R, \quad (3.17)$$

where we have introduced the R-symmetry breaking scale $f_R = O(\Lambda_{\text{dyn}})$ and define the R-symmetry so that $\langle S_0 \rangle > 0$. At this vacuum, the scalar component of S_0 is decomposed into a flaton s and the R-axion a by,

$$S_0 = \frac{1}{\sqrt{2}} (f_R + s) e^{ia/f_R}. \quad (3.18)$$

Then, the mass of the flaton is given by,

$$m_s = 4\sqrt{2} \frac{\lambda \Lambda_{\text{dyn}}^2 \Lambda_4^3}{(4\Lambda_4^4 + \Lambda_6^4)} \simeq \sqrt{2} \frac{\lambda \Lambda_{\text{dyn}}^2}{\Lambda_4} \simeq \sqrt{2} \frac{c_4}{4\pi} \lambda \Lambda_{\text{dyn}}, \quad (3.19)$$

where we have used $F_{S_0} = \lambda \Lambda_{\text{dyn}}^2$ and assumed eq. (3.16) with $c_4 = c_6 = O(1)$. Therefore, the flaton can be in a TeV range for $\lambda \sim 1$ and $c_4 \sim 1$, which is a crucial property for the flaton to make the narrow resonance appropriate for the dark matter annihilation.

On the other hand, the R-axion mass is much more suppressed and mainly comes from the constant term in the superpotential which breaks the R-symmetry explicitly.³

³In this study, we assume that the messenger sector of the gauge mediation also respects the R-symmetry. Otherwise, the radiative correction to the Kähler potential of S_0 from the messenger sector gives rise to the dominant contribution to the R-axion mass. The R-breaking mass from the Higgs sector, on the other hand, is smaller than the one in eq. (3.20), even if the so-called μ -term does not respect the R-symmetry.

In the supergravity with (almost) vanishing cosmological constant, the R-axion acquires a small mass [23],

$$m_{\text{axion}}^2 \sim \frac{m_{3/2} F_{S_0}}{f_R}. \quad (3.20)$$

In the case of the low-scale gauge mediation with the dynamical SUSY breaking scale around 30 TeV, the R-axion mass is tens to hundreds of MeV range.

3.3.2 Spectrum and interactions of light particles

The spectrum of other light particles becomes also complicated in the presence of the R-symmetry breaking, since S_a and M_a scalars mix with each other via a cross term in the F -term potential $|m_{S_a} S_a - \lambda S_0 M_a|^2$. To analyze the mass spectrum and interactions of those particles, we decompose M_a and S_a as

$$\begin{aligned} S_a &= \frac{1}{\sqrt{2}}(x_s + i y_s)e^{ia/f_R}, \\ M_a &= \frac{1}{\sqrt{2}}(x_m + i y_m). \end{aligned} \quad (3.21)$$

Here, we have suppressed the index a , since the particles with different values of a decouple from each other in the following analysis.

By using this expressions, we obtain a scalar potential,

$$\begin{aligned} V &= |\lambda' \Lambda_{\text{dyn}} M_a|^2 + \left| \lambda \Lambda_{\text{dyn}}^2 - \frac{\lambda}{2} M_a^2 \right|^2 + |\lambda S_0 M_a + \lambda' \Lambda_{\text{dyn}} S_a|^2, \\ &= \frac{1}{2} \left((\lambda'^2 - \lambda^2) \Lambda_{\text{dyn}}^2 + \frac{\lambda^2}{2} (s + f_R)^2 \right) x_m^2 + \frac{1}{2} \left((\lambda'^2 + \lambda^2) \Lambda_{\text{dyn}}^2 + \frac{\lambda^2}{2} (s + f_R)^2 \right) y_m^2 \\ &\quad + \frac{1}{2} \lambda'^2 \Lambda_{\text{dyn}}^2 x_s^2 + \frac{1}{2} \lambda'^2 \Lambda_{\text{dyn}}^2 y_s^2 + \frac{\lambda \lambda'}{\sqrt{2}} \Lambda_{\text{dyn}} (s + f_R) x_m x_s + \frac{\lambda \lambda'}{\sqrt{2}} \Lambda_{\text{dyn}} (s + f_R) y_m y_s \\ &\quad + \lambda^2 \Lambda_{\text{dyn}}^4 + \frac{\lambda^2}{24} (x_m^2 + y_m^2)^2. \end{aligned} \quad (3.22)$$

Notice that the R-axion does not show up in the scalar interactions in this basis, and it only appears in the derivative couplings. From this potential, we find that the pseudo-Nambu-Goldstone mode resides not in (y_m, y_s) but in (x_m, x_s) . In the following, we concentrate on the real parts (x_m, x_s) .

The mass-squared matrix of (x_m, x_s) is given by,

$$M^2 = \begin{pmatrix} (\lambda'^2 - \lambda^2) \Lambda_{\text{dyn}}^2 + \lambda^2 \langle S_0 \rangle^2 & \lambda \lambda' \Lambda_{\text{dyn}} \langle S_0 \rangle \\ \lambda \lambda' \Lambda_{\text{dyn}} \langle S_0 \rangle & \lambda'^2 \Lambda_{\text{dyn}}^2 \end{pmatrix}, \quad (3.23)$$

and hence, the masses of the eigenmodes (ϕ, H) are;

$$m_\phi^2 = \frac{1}{2} \left(\text{tr } M^2 - \sqrt{(\text{tr } M^2)^2 - 4 \det M^2} \right) = \frac{\det M^2}{m_H^2}, \quad (3.24)$$

$$m_H^2 = \frac{1}{2} \left(\text{tr } M^2 + \sqrt{(\text{tr } M^2)^2 - 4 \det M^2} \right), \quad (3.25)$$

$$\text{tr } M^2 = (2\lambda'^2 - \lambda^2) \Lambda_{\text{dyn}}^2 + \lambda^2 \langle S_0 \rangle^2, \quad (3.26)$$

$$\det M^2 = \lambda'^2 (\lambda'^2 - \lambda^2) \Lambda_{\text{dyn}}^4. \quad (3.27)$$

The mixing angle is given by,

$$\begin{aligned} x_m &= \cos \theta \phi - \sin \theta H, \\ x_s &= \sin \theta \phi + \cos \theta H, \end{aligned} \tag{3.28}$$

with

$$\begin{aligned} \tan \theta &= -\frac{\lambda \lambda' \Lambda_{\text{dyn}} \langle S_0 \rangle}{\lambda'^2 \Lambda_{\text{dyn}}^2 - m_\phi^2}, \\ \sin \theta \cos \theta &= -\frac{\lambda \lambda' \Lambda_{\text{dyn}} \langle S_0 \rangle}{m_H^2 - m_\phi^2}. \end{aligned} \tag{3.29}$$

As a result, we find that the lighter scalar ϕ denotes the Nambu-Goldstone mode in the limit of $\lambda = \lambda'$, and hence, we consider ϕ as the dark matter.

The R-axion interactions only appear in the kinetic terms. In the basis we have defined, the R-axion interaction comes from the kinetic terms of S_0 and S_a ,

$$\mathcal{L} = \frac{1}{2}(\partial a)^2 \left(1 + \frac{s}{f_R}\right)^2 + \frac{1}{2f_R^2}(\partial a)^2(x_s^2 + y_s^2) + \frac{1}{f_R}\partial_\mu a(x_s\partial^\mu y_s - y_s\partial^\mu x_s). \tag{3.30}$$

Altogether, in the Nambu-Goldstone dark matter scenario (i.e., $\lambda' - \lambda \ll 1$), light particles sector consists of the dark matter and the flaton in a TeV range, and the gravitino and the R-axion with much smaller masses, while the other components in S_a and M_a have masses of the order of the SUSY breaking scale. The most relevant terms for the dark matter annihilation is, then, given by,

$$\mathcal{L}_{\text{int}} = \frac{\lambda^2}{2}f_R\frac{m_\phi^2}{m_H^2 - m_\phi^2}s\phi^2 + \frac{1}{2}(\partial a)^2\left(1 + \frac{s}{f_R}\right)^2, \tag{3.31}$$

where the first term comes from the scalar potential in eq. (3.22), while the second term comes from eq. (3.30).

3.3.3 Flaton decay

In order to discuss the dark matter annihilation via the s -channel exchange of the flaton, it is important to know the decay properties of the flaton. In particular, the decay rate into a dark matter pair is important even if the pole is unphysical, i.e., $2m_\phi > m_s$, since the decay rate must be defined not on the exact pole, but on the center of mass energy of the dark matter collision, E_{CM} .

First, we consider the decay mode into a pair of the R-axions. The relevant interactions of the decay comes from the first term in eq. (3.31), and the decay rate into a pair of the R-axion is given by,

$$\Gamma_{s \rightarrow aa} = \frac{1}{32\pi} \frac{m_s^3}{f_R^2}, \tag{3.32}$$

where we have neglected the mass of the R-axion and taken the final state velocity to be $\beta_f = 1$. For example, the decay rate is very small, i.e., $\Gamma/m \lesssim 10^{-4}$ for $f_R \gtrsim 30$ TeV and

$m_s = 2 \text{ TeV}$. As we will see this is favorable to realize a large effective boost factor via the Breit-Wigner enhancement.

Next, we consider the flaton decay into a pair of the dark matter. The relevant interaction term is given in eq. (3.31) and the resultant decay rate is given by,

$$\Gamma_{s \rightarrow \phi\phi} = \frac{\beta_\phi}{32\pi} \frac{\lambda^4 f_R^2}{m_s^2} \left(\frac{m_\phi^2}{m_H^2 - m_\phi^2} \right)^2 m_s, \quad (3.33)$$

where β_ϕ denotes the size of the velocity of the dark matter. Notice that the value of $\Gamma_{s \rightarrow \phi\phi}/\beta_\phi$ is well-defined even in the unphysical region, i.e., $2m_\phi > m_s$. The value of $\Gamma_{s \rightarrow \phi\phi}/\beta_\phi$ is at most comparative to $\Gamma_{s \rightarrow aa}$,

$$\Gamma_{s \rightarrow \phi\phi} \simeq \frac{\beta_\phi}{512\pi} \left(\frac{\lambda f_R}{m_H} \right)^4 \frac{m_s^3}{f_R^2}, \quad (3.34)$$

where we have used $m_\phi \simeq m_s/2$ and $m_H \gg m_\phi$. Therefore, we find that the decay rate into a dark matter pair does not dominate over the one into an R-axion pair.

Let us also consider the flaton decay into a pair of the gravitinos. The relevant interaction comes from the higher dimensional terms in the Kähler potential eq. (3.15), and the resultant interaction term is given by,

$$\mathcal{L}_{\text{int}} \sim \frac{F_{S_0}}{\Lambda_4^2} s \psi \psi + h.c. = \frac{m_s^2}{F_{S_0}} s \psi \psi + h.c., \quad (3.35)$$

where we have used eq. (3.19), i.e., $\Lambda_4 \sim F_{S_0}/m_s$. Therefore, the decay width is suppressed by $(m_s/\Lambda_{\text{SUSY}})^4$, and hence, this mode is further suppressed compared with the mode into an R-axion pair.

Putting them all together, we obtain the flaton decay width at $E_{\text{CM}} \simeq m_s$,

$$\Gamma_s(E_{\text{CM}}) = \Gamma_{s \rightarrow aa} + \Gamma_{s \rightarrow \phi\phi} + \dots \quad (3.36)$$

where $E_{\text{CM}} > 2m_\phi$, and the dots refer to the modes into the MSSM particles (see appendix C). In the following analysis, we approximate the above decay rate by,

$$\Gamma_s(E_{\text{CM}}) \simeq \Gamma_s(m_s) \simeq \Gamma_{s \rightarrow aa}, \quad (3.37)$$

since all the other modes are subdominant at $E_{\text{CM}} \simeq m_s$.

3.3.4 Dark matter annihilation via the s -channel flaton

Now, let us consider the dark matter annihilation via the s -channel flaton exchange. The relevant interactions are again given in eq. (3.31). The amplitude of this process is given by

$$\mathcal{M} = \lambda^2 \frac{m_\phi^2}{m_H^2 - m_\phi^2} \frac{E_{\text{CM}}^2}{E_{\text{CM}}^2 - m_s^2 + im_s \Gamma_s(E_{\text{CM}})}, \quad (3.38)$$

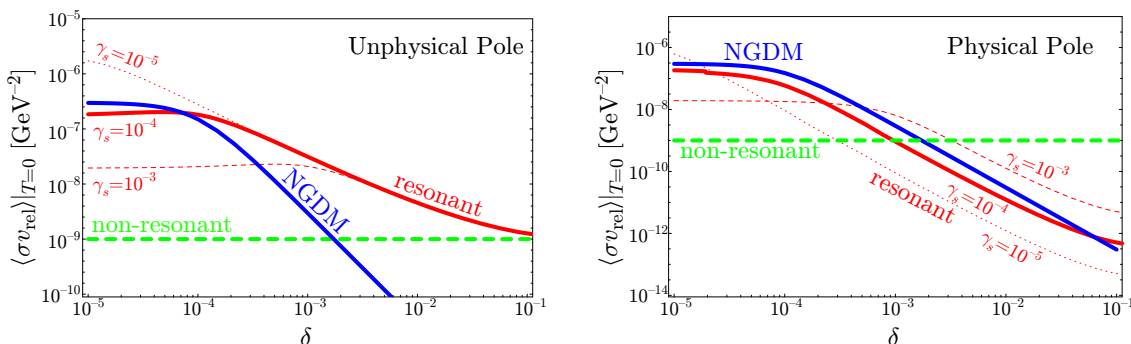


Figure 1. Left) The δ dependence of the required annihilation cross section at zero temperature from the observed dark matter density in the case of the unphysical pole. The red lines correspond to $\gamma_s = 10^{-3}$, $\gamma_s = 10^{-4}$ and $\gamma_s = 10^{-5}$ from bottom to top. The green line shows the required annihilation cross section in the usual thermal history. The blue line shows the predicted annihilation cross section for $\lambda = 0.84$, $m_H = 30$ TeV and $m_\phi = 1$ TeV. Right) The required annihilation cross section in the case of the physical pole.

and the cross section by

$$\begin{aligned} \sigma v_{\text{rel}} &= \frac{v_{\text{rel}}}{32\pi} \frac{\beta_f}{\beta_\phi} \left(\frac{m_\phi^2}{m_H^2 - m_\phi^2} \right)^2 \frac{\lambda^4 E_{\text{CM}}^2}{(E_{\text{CM}}^2 - m_s^2)^2 + m_s^2 \Gamma_s^2} \\ &\simeq \frac{\lambda^4}{64\pi} \left(\frac{m_\phi}{m_H} \right)^4 \frac{1}{m_\phi^2} \frac{1}{(\delta + v_{\text{rel}}^2/4)^2 + \gamma_s^2}, \end{aligned} \quad (3.39)$$

where the Γ_s and β_ϕ are defined at $E_{\text{CM}} > 2m_\phi$. In the final expression, we have used the non-relativistic approximation,

$$E_{\text{CM}}^2 = 4m_\phi^2 + m_\phi^2 v_{\text{rel}}^2, \quad (3.40)$$

and introduced parameters δ and γ_s by

$$m_s^2 = 4m_\phi^2(1 - \delta), \quad \gamma_s = \Gamma_s/m_s. \quad (3.41)$$

From this expression, we find that the annihilation cross section of the dark matter is substantially enhanced compared with the one given in eq. (3.14), for $|\delta|, \gamma_s \ll 1$, which allows a sufficient annihilation cross section to reproduce the observed dark matter density.

3.3.5 Dark matter density and Breit-Wigner enhancement

Although we obtained the enhanced annihilation cross section of the dark matter, we should note that the thermal history of the dark matter density is drastically changed from the usual thermal relic density when the dark matter annihilates via the narrow resonance [24, 25], and hence, the required annihilation cross section is different from the value given in eq. (2.4). Instead, in terms of the annihilation cross section at the zero temperature, the required annihilation cross section to obtain the correct abundance is given by [11],

$$\langle \sigma v_{\text{rel}} \rangle|_{T=0} \sim 10^{-9} \text{ GeV}^{-2} \times \frac{x_b}{x_f}. \quad (3.42)$$

Here $x_f \simeq 20$ denotes the freeze-out parameter of the usual (non-resonant) thermal freeze-out history, while x_b is defined by,

$$\frac{1}{x_b} \simeq \frac{1}{\langle \sigma v_{\text{rel}} \rangle |_{T=0}} \int_{x_f}^{\infty} \frac{\langle \sigma v_{\text{rel}} \rangle}{x^2} dx. \quad (3.43)$$

In the case of the unphysical pole, i.e., $m_s < 2m_\phi$, x_b is well approximated by $\min[\delta^{-1}, \gamma_s^{-1}]$, and the above required annihilation cross section at the zero temperature is simply given by,

$$\langle \sigma v_{\text{rel}} \rangle |_{T=0} \sim 10^{-9} \text{ GeV}^{-2} \times \frac{1}{x_f \text{Max}[\delta, \gamma_s]}. \quad (3.44)$$

In figure 1, we show the required annihilation cross section for given parameters as red lines. The figure shows that eq. (3.44) gives a good approximation.

On the other hand, in the case of the physical pole, the estimation of x_b is much more complicated. In particular, the thermal average picks up the pole at $v_{\text{rel}}^2 = 4|\delta|$ when the temperature is rather high, i.e., $x^{-1} \gg |\delta|$, and hence, the annihilation cross section can be higher at the higher temperature than the one at the zero temperature. As a result, the required annihilation cross section at the zero temperature can be much lower than the one in the usual thermal relic history. In figure 1, we also show the required cross section at the zero temperature in the case of the physical pole. The figure shows that the required cross section can be lower than the usual value.

Now, let us compare these values with the dark matter annihilation cross section given in eq. (3.39). For example, if we take, $m_\phi = 1 \text{ TeV}$, $f_R = 30 \text{ TeV}$, $m_H = 30 \text{ TeV}$ and $\lambda = 1$, the decay rate is very small $\gamma_s \simeq 10^{-4}$. In this case, the cross section at the zero temperature is

$$\langle \sigma v_{\text{rel}} \rangle |_{T=0} \simeq 3 \times 10^{-15} \text{ GeV}^{-2} \times \frac{\lambda^4}{\delta^2 + \gamma_s^2} \left(\frac{m_\phi}{1 \text{ TeV}} \right)^2 \left(\frac{30 \text{ TeV}}{m_H} \right)^4. \quad (3.45)$$

In figure 1, we show the predicted annihilation cross section. From the figure, we find that the required annihilation cross section is achieved at

$$\begin{aligned} \delta &\sim 10^{-4}, & (\text{for unphysical pole}), \\ \delta &\sim -10^{-1}, & (\text{for physical pole}), \end{aligned} \quad (3.46)$$

for the given parameter set ($\lambda = 1$, $m_\phi = 1 \text{ TeV}$, and $m_H = f_R = 30 \text{ TeV}$). Therefore, the Nambu-Goldstone dark matter is consistent with the observed dark matter density when it annihilates via the flaton resonance with the values of δ given above.

Interestingly, the Nambu-Goldstone dark matter predicts a non-trivial effective boost factor. The effective boost factor in the Breit-Wigner enhancement is defined by,

$$\text{BF} = \frac{x_b}{x_f}. \quad (3.47)$$

Thus, the effective boost factor for the above two solutions are given by,

$$\begin{aligned} \text{BF} &\sim 10^2, & (\text{for unphysical pole}), \\ \text{BF} &\sim 10^{-3}, & (\text{for physical pole}), \end{aligned} \tag{3.48}$$

respectively for the parameters given above.

Therefore, we find that the Nambu-Goldstone dark matter model predicts a non-trivial effective boost factor. Especially, the model with the unphysical flaton pole ($m_s < 2m_\phi$) is strongly favored in the light of the recent cosmic ray experiments. In this case, the parameter dependence of the boost factor is simply given by,

$$\text{BF} \sim 10^2 \times \lambda^4 \left(\frac{m_\phi}{1 \text{ TeV}} \right)^2 \left(\frac{30 \text{ TeV}}{m_H} \right)^4. \tag{3.49}$$

Here, we have used eqs. (3.39) and (3.45).

3.3.6 R-axion decay and anti-proton flux

As we have discussed, the dark matter dominantly annihilates into an R-axion pair via the flaton resonance. Interestingly, since the R-axion has a mass in the range of tens to hundreds of MeV, it mainly decays into light lepton pairs (see ref. [26] for detailed discussion on the R-axion properties).

Therefore, the Nambu-Goldstone dark matter model provides a concrete example of the scenario developed in ref. [14]. There, the dark matter annihilate into a new light particle which subsequently decays into light leptons. In this way, we can obtain a hard positron spectrum without any additional anti-protons, so that we can explain the PAMELA results consistently.

Here, we comment on the constraints on the decay constant and mass of the R-axion. For the R-axion in a mass range between two electrons and two muons, the stringent constraint comes from a beam-dump experiment [30], which constrains the decay constant as

$$f_R \gtrsim 10^{4.5} \text{ GeV} \times \left(\frac{m_a}{10 \text{ MeV}} \right)^{1/2}, \tag{3.50}$$

when we assume that the Higgs sector respects the R-symmetry and the R-charge of the so-called μ -term, $H_u H_d$, is two [26]. Thus, our choice of the scales of the R-symmetry breaking and the SUSY breaking in the previous discussion are marginally consistent with the constraint.⁴ On the other hand, for the R-axion heavier than two muons, the most stringent constraint comes from the rare decay of the Υ meson, $Br(\Upsilon \rightarrow \gamma + a) < 10^{-(5-6)}$ [31], which is given by $f_R \gtrsim 10^3 \text{ GeV}$. Furthermore, since we are considering the R-axion with mass heavier than a few tens of MeV, it is free from the astrophysical constraints.⁵

⁴For other choices of the R-charge of the μ -term, the constraint can be changed. For example, when the R-charge of the μ -term is zero, the R-axion does not mix with the neutral Higgs bosons in the SSM. In this case, the couplings between the R-axion and the SM fermion vanish at the tree-level, and hence, the above constraint on the decay constant is weakened. We may also consider the Higgs sector without the R-symmetry. In that case, the degree of the mixing between the R-axion and the Higgs bosons is also altered from the one discussed in ref. [26], which may weaken the above constraint.

⁵As discussed in ref. [26], the R-axion can be detected at the LHC experiment if the decay constant is in tens of TeV range which makes the R-axion mainly decay into a muon pair.

4 Conclusion

In this paper, we have revisited the possibility of the dark matter in the SUSY breaking sector, in the light of the recent cosmic ray experiments. In our model, the dark matter is identified as a pseudo-Nambu-Goldstone mode in the SUSY breaking sector with a mass in a TeV range which makes it possible to interpret the observed bump in the $e^+ + e^-$ flux at ATIC/PPB-BETS experiments. Interestingly, the observed dark matter density requires an existence of a narrow resonance through which the dark matter annihilates, which results in a large effective boost factor (in the case of the unphysical pole). In addition, the dominant final state of the annihilation process is a pair of the R-axions each of which decays into a pair of light leptons. Therefore, the Nambu-Goldstone dark matter model is quite favorable to explain the PAMELA anomaly.

Several comments are in order. In the model of the Nambu-Goldstone dark matter, the SUSY breaking scale is around 30 TeV. Thus, the model is accompanied by the gravitino with a mass in a ten eV range. The gravitino with such a small mass is attractive, since it causes no problem in cosmology and astrophysics [27, 28].

In the Nambu-Goldstone dark matter scenario, the dark matter mass is controlled by the degree of the explicit breaking of the approximate global $SO(6)$ symmetry, i.e., the difference between λ and λ' (see eq. (3.6)). One may attribute the origin of the tuning between λ and λ' to a conformal dynamics at high energy scales. As discussed in ref. [29], the conformal extensions of the vector-like SUSY breaking model possess an IR-fixed point where the global symmetry is enhanced. In such models, even if $|\lambda' - \lambda| = O(1)$ at a high energy scale, the couplings flow to the IR-fixed point in the course of the renormalization group evolution and end up with $|\lambda - \lambda'| \ll 1$, at the scale of the SUSY breaking. Thus, if we assume that the SUSY breaking sector was in a conformal regime at higher energy scales than the SUSY breaking scale, we can explain the lightness of the dark matter compared with the scale of the SUSY breaking.

Acknowledgments

The work of M. I. was supported by the U.S. Department of Energy under contract number DE-AC02-76SF00515. The research of Y. N. is supported in part by NSF grant PHY-0555662 and the UC Berkeley Center for Theoretical Physics. The work of H.M. and T.T.Y. was supported in part by World Premier International Research Center Initiative (WPI Initiative), MEXT, Japan. The work of H.M. was also supported in part by the U.S. DOE under Contract DE-AC03-76SF00098, and in part by the NSF under grant PHY-04-57315.

A Coleman-Weinberg potential of IYIT model

Here, we show the detailed analysis of the Coleman-Weinberg potential of the flaton S_0 (see also ref. [32].) The classical flat direction S_0 is lifted by a one-loop correction via the interaction $W = \lambda S_0 M_a^2$. Using the notation $\sigma = \lambda S_0$, $x = \lambda' \Lambda_{\text{dyn}}$, $y = \lambda \Lambda_{\text{dyn}}$, the mass

matrix for the fermions is

$$M_f = \begin{pmatrix} -\sigma & x \\ x & 0 \end{pmatrix} \quad (\text{A.1})$$

and for the bosons

$$M_b^2 = \begin{pmatrix} x^2 + \sigma^2 & -x\sigma & -y^2 & 0 \\ -x\sigma & x^2 & 0 & 0 \\ -y^2 & 0 & x^2 + \sigma^2 & -x\sigma \\ 0 & 0 & -x\sigma & x^2 \end{pmatrix} \quad (\text{A.2})$$

The eigenvalues of the fermion mass-squared matrix are

$$m_f^2 = \frac{1}{2} \left(2x^2 + \sigma^2 \pm \sigma \sqrt{4x^2 + \sigma^2} \right), \quad (\text{A.3})$$

while for bosons

$$m_b^2 = \frac{1}{2} \left(2x^2 + \sigma^2 - y^2 \pm \sqrt{4x^2\sigma^2 + \sigma^4 - 2y^2\sigma^2 + y^4} \right), \quad (\text{A.4})$$

$$\frac{1}{2} \left(2x^2 + \sigma^2 + y^2 \pm \sqrt{4x^2\sigma^2 + \sigma^4 + 2y^2\sigma^2 + y^4} \right). \quad (\text{A.5})$$

Using this spectrum, we can compute the Coleman-Weinberg potential.

$$\Delta V_{CW} = \frac{5}{64\pi^2} \text{STr } m^4 \ln m^2, \quad (\text{A.6})$$

where a factor 5 comes from the number of M_a . Expanding it up to second order in σ , we obtain

$$\begin{aligned} \text{STr } m^4 \ln m^2 &= -4x^4 \ln x + (x^2 - y^2)^2 \ln(x^2 - y^2) + (x^2 + y^2)^2 \log(x^2 + y^2) \\ &+ \frac{2}{y^2} \left((x^2 + y^2)^2 \log(x^2 + y^2) - (x^2 - y^2)^2 \log(x^2 - y^2) \right) \\ &- 4x^2 y^2 \log(x^2) - 2x^2 y^2 \sigma^2 + O(\sigma^4). \end{aligned} \quad (\text{A.7})$$

Since $y < x$ is needed to avoid tachyon, we take the small y limit as

$$\text{STr } m^4 \ln m^2 = y^4(3 + 4 \log(x)) + \frac{4y^4}{3x^2} \sigma^2, \quad (\text{A.8})$$

which is a good approximation even as $y \rightarrow x$. Within this approximation, the mass term for S_0 from the Coleman-Weinberg potential is

$$\Delta V_{CW} = \frac{5}{64\pi^2} \frac{4(\lambda \Lambda_{\text{dyn}})^4}{3(\lambda' \Lambda_{\text{dyn}})^2} |\lambda S|^2 = \frac{5}{3(4\pi)^2} \frac{\lambda^6}{\lambda'^2} \Lambda_{\text{dyn}}^2 |S_0|^2. \quad (\text{A.9})$$

Therefore, we obtain the mass of the flat direction,⁶

$$m_{S_0} \simeq \sqrt{\frac{5}{3}} \frac{\lambda^3}{(4\pi) \lambda'} \Lambda_{\text{dyn}}. \quad (\text{A.11})$$

⁶Corresponding Kähler potential corrections to reproduce ΔV_{CW} is given by

$$\Delta K = -\frac{5}{3(4\pi)^2} \frac{\lambda^4}{4\lambda'^2 \Lambda_{\text{dyn}}^2} (S_0^\dagger S_0)^2. \quad (\text{A.10})$$

Notice that the flat direction is also lifted by higher dimensional terms of S_0 in the Kähler potential which is suppressed by the dynamical scale $4\pi\Lambda_{\text{dyn}}$. However, the flat direction mass is dominated by the one-loop contribution analyzed here, since the fields circulating in the loop is much lighter than $4\pi\Lambda_{\text{dyn}}$.

B R-breaking in gauged IYIT model

In the main text, we have discussed how R-symmetry breaking in the hidden sector drastically changes the decay process of SSDM scenario. In this appendix, we study the R-symmetry breaking of the IYIT model with additional U(1) gauge symmetry. We embed $\text{SO}(2) \times \text{SO}(4)$ in the original $\text{SO}(6)$ global symmetry of the IYIT model, where $\text{SO}(2) = \text{U}(1)$ is gauged. The dark matter candidate M_a lies in vector representation of $\text{SO}(4)$ ($a = 1, \dots, 4$).

The low-energy effective superpotential of the gauged IYIT model is given by⁷

$$W = xS_+M_- + xS_-M_+ + yS_aM_a \tag{B.1}$$

with the constraint $M_+M_- + \frac{1}{2}M_aM_a - \Lambda_{\text{dyn}}^2 = 0$. The subscript \pm denotes the U(1) charge of the chiral superfields. We parametrize the solution of the deformed moduli constraint as

$$M_+ = \Lambda_{\text{dyn}} e^{\phi/\sqrt{2}\Lambda_{\text{dyn}}}, \quad M_- = \Lambda_{\text{dyn}} e^{-\phi/\sqrt{2}\Lambda_{\text{dyn}}} \tag{B.2}$$

In these variables, the leading order Kähler potential is canonically normalized:

$$K = |S_+|^2 + |S_-|^2 + |\phi|^2 + \sum_a (|M_a|^2 + |S_a|^2) + \dots \tag{B.3}$$

where non-canonical Kähler potential may be neglected when $F_{S_{\pm}} = \lambda\Lambda_{\text{dyn}}^2 \ll \Lambda_{\text{dyn}}^2$. On the other hand, the superpotential can be written as

$$W = mv \left(S_+ e^{-\phi/\sqrt{2}\Lambda_{\text{dyn}}} + S_- e^{\phi/\sqrt{2}\Lambda_{\text{dyn}}} \right) \sqrt{\Lambda_{\text{dyn}}^2 - \frac{1}{2}M_aM_a} \tag{B.4}$$

The tree level vacua have moduli space spanned by $\phi = M_a = S_a = 0$, $S_+ = S_- = \sigma$. At the tree level, massless degrees of freedom are one R-axion, one real modulus $\sigma = (\text{Re}[S_+] + \text{Re}[S_-])/2$ and one goldstino after gauging away the U(1) Nambu-Goldstone boson at generic points of the moduli space. The R-axion remains massless in the field theory limit, while the pseudo-modulus σ will acquire a quantum potential, whose shape and resulting VEV determines whether the R-symmetry is broken.

To see the R-symmetry breaking, we compute the Coleman-Weinberg potential $V(\sigma) = (1/64\pi^2) \text{STr } m^4(\sigma) \log m^2(\sigma)$. In figure 2, we plot the Coleman-Weinberg potential for a given U(1) gauge coupling constant. The figure shows that the symmetry enhancement point $\sigma = 0$ becomes the local maximum and the Coleman-Weinberg potential develops a minimum at $\sigma \neq 0$ for a larger value of the additional gauge coupling constant. Thus, our U(1) gauged IYIT model serves as a perturbative model of R-breaking hidden sector with hidden dark matter. The R-breaking depends on the U(1) coupling constant.

⁷When we set $M_a = S_a = 0$, our model is equivalent to $k \rightarrow \infty$ limit of the model with $W = xS_+M_- + xS_-M_+ + kX(M_+M_- - \Lambda_{\text{dyn}}^2)$ which was studied in [22].

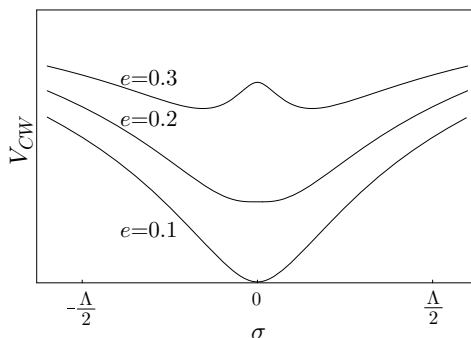


Figure 2. The Coleman-Weinberg potential for the U(1) gauged IYIT model. In the figure, we have assumed $\lambda = 0.5$, $\lambda' = 1$, and the gauge coupling constant as shown in the figure.

C F-flaton decay into the SSM particle

In this appendix, we consider the decay modes of the flaton into the SSM particles. Since we are assuming the model with gauge mediation, the flaton couples to the SSM fields as the results of the mediation effects. For example, the effective coupling between the flaton and the gauginos is given by a Yukawa interaction;

$$\mathcal{L}_{\text{eff}} \simeq \frac{1}{2} \frac{m_i}{f_R} \left(1 + O\left(\frac{f_R^2}{F_{S_0}}\right) \right) s \lambda^i \lambda^i + h.c., \tag{C.1}$$

where m_i denotes the gaugino mass and i runs the SSM gauge groups. Notice that the leading term in the above effective coupling is model independent as long as the messenger sector possesses the R-symmetry. On the other hand, the coupling between the flaton and the sfermions depends on the messenger sector even if it is R-symmetric, and is given by,

$$\mathcal{L}_{\text{eff}} = \left. \frac{\partial m_{\tilde{f}}^2}{\partial s} \right|_{s=0} \times s \tilde{f} \tilde{f}, \tag{C.2}$$

where the model dependent coefficient $\partial m_{\tilde{f}}^2 / \partial s$ satisfies

$$\left. \frac{\partial m_{\tilde{f}}^2}{\partial s} \right|_{s=0} \leq \frac{m_{\tilde{f}}^2}{f_R}. \tag{C.3}$$

From these interactions, the flaton decays into a pair of the SSM particles. For instance, the decay rate into a pair of the gluinos are given by

$$\Gamma_{s \rightarrow \tilde{g}\tilde{g}} \simeq \frac{1}{4\pi} \left(\frac{m_{\tilde{g}}}{m_s} \right)^2 \frac{m_s^3}{f_R^2}. \tag{C.4}$$

Therefore, depending on the spectrum of the SSM and the dark matter ($m_{\text{DM}} \simeq m_s/2$), the branching ratio of the flaton into the SSM particles can be suppressed. Notice that the branching ratio into the gravitino pair is highly suppressed [33].

References

- [1] J. Chang et al., *An excess of cosmic ray electrons at energies of 300.800 GeV*, *Nature* **456** (2008) 362 [SPIRES].
- [2] PPB-BETS collaboration, S. Torii et al., *High-energy electron observations by PPB-BETS flight in Antarctica*, [arXiv:0809.0760](#) [SPIRES].
- [3] D. Hooper, P. Blasi and P.D. Serpico, *Pulsars as the sources of high energy cosmic ray positrons*, *JCAP* **01** (2009) 025 [[arXiv:0810.1527](#)] [SPIRES].
- [4] H. Yuksel, M.D. Kistler and T. Stanev, *TeV gamma rays from Geminga and the origin of the GeV positron excess*, [arXiv:0810.2784](#) [SPIRES].
- [5] S. Profumo, *Dissecting Pamela (and ATIC) with Occam's razor: existing, well-known pulsars naturally account for the "anomalous" cosmic-ray electron and positron data*, [arXiv:0812.4457](#) [SPIRES].
- [6] N.J. Shaviv, E. Nakar and T. Piran, *Natural explanation for the anomalous positron to electron ratio with supernova remnants as the sole cosmic ray source*, [arXiv:0902.0376](#) [SPIRES] and references therein.
- [7] PAMELA collaboration, O. Adriani et al., *An anomalous positron abundance in cosmic rays with energies 1.5-100 GeV*, *Nature* **458** (2009) 607 [[arXiv:0810.4995](#)] [SPIRES].
- [8] See, H. Murayama, *Physics beyond the standard model and dark matter*, [arXiv:0704.2276](#) [SPIRES].
- [9] S. Dimopoulos, G.F. Giudice and A. Pomarol, *Dark matter in theories of gauge-mediated supersymmetry breaking*, *Phys. Lett. B* **389** (1996) 37 [[hep-ph/9607225](#)] [SPIRES].
- [10] WMAP collaboration, E. Komatsu et al., *Five-year Wilkinson Microwave Anisotropy Probe (WMAP) observations: cosmological interpretation*, *Astrophys. J. Suppl.* **180** (2009) 330 [[arXiv:0803.0547](#)] [SPIRES].
- [11] M. Ibe, H. Murayama and T.T. Yanagida, *Breit-Wigner enhancement of dark matter annihilation*, [arXiv:0812.0072](#) [SPIRES].
- [12] M. Pospelov and A. Ritz, *Astrophysical signatures of secluded dark matter*, *Phys. Lett. B* **671** (2009) 391 [[arXiv:0810.1502](#)] [SPIRES].
- [13] D. Feldman, Z. Liu and P. Nath, *PAMELA positron excess as a signal from the hidden sector*, *Phys. Rev. D* **79** (2009) 063509 [[arXiv:0810.5762](#)] [SPIRES].
- [14] I. Cholis, D.P. Finkbeiner, L. Goodenough and N. Weiner, *The PAMELA positron excess from annihilations into a light boson*, [arXiv:0810.5344](#) [SPIRES].
- [15] Y. Nomura and J. Thaler, *Dark matter through the axion portal*, [arXiv:0810.5397](#) [SPIRES].
- [16] M. Dine, W. Fischler and M. Srednicki, *Supersymmetric technicolor*, *Nucl. Phys. B* **189** (1981) 575 [SPIRES];
S. Dimopoulos and S. Raby, *Supercolor*, *Nucl. Phys. B* **192** (1981) 353 [SPIRES];
M. Dine and W. Fischler, *A phenomenological model of particle physics based on supersymmetry*, *Phys. Lett. B* **110** (1982) 227 [SPIRES]; *A supersymmetric gut*, *Nucl. Phys. B* **204** (1982) 346 [SPIRES];
C.R. Nappi and B.A. Ovrut, *Supersymmetric extension of the SU(3) × SU(2) × U(1) model*, *Phys. Lett. B* **113** (1982) 175 [SPIRES];
L. Alvarez-Gaume, M. Claudson and M.B. Wise, *Low-energy supersymmetry*, *Nucl. Phys. B* **207** (1982) 96 [SPIRES];

- S. Dimopoulos and S. Raby, *Geometric hierarchy*, *Nucl. Phys. B* **219** (1983) 479 [SPIRES].
- [17] M. Dine and A.E. Nelson, *Dynamical supersymmetry breaking at low-energies*, *Phys. Rev. D* **48** (1993) 1277 [hep-ph/9303230] [SPIRES].
- [18] M. Dine, A.E. Nelson and Y. Shirman, *Low-energy dynamical supersymmetry breaking simplified*, *Phys. Rev. D* **51** (1995) 1362 [hep-ph/9408384] [SPIRES].
- [19] M. Dine, A.E. Nelson, Y. Nir and Y. Shirman, *New tools for low-energy dynamical supersymmetry breaking*, *Phys. Rev. D* **53** (1996) 2658 [hep-ph/9507378] [SPIRES].
- [20] K.-I. Izawa and T. Yanagida, *Dynamical supersymmetry breaking in vector-like gauge theories*, *Prog. Theor. Phys.* **95** (1996) 829 [hep-th/9602180] [SPIRES];
K.A. Intriligator and S.D. Thomas, *Dynamical supersymmetry breaking on quantum moduli spaces*, *Nucl. Phys. B* **473** (1996) 121 [hep-th/9603158] [SPIRES].
- [21] M.A. Luty, *Naive dimensional analysis and supersymmetry*, *Phys. Rev. D* **57** (1998) 1531 [hep-ph/9706235] [SPIRES];
A.G. Cohen, D.B. Kaplan and A.E. Nelson, *Counting 4π 's in strongly coupled supersymmetry*, *Phys. Lett. B* **412** (1997) 301 [hep-ph/9706275] [SPIRES].
- [22] M. Dine and J. Mason, *Gauge mediation in metastable vacua*, *Phys. Rev. D* **77** (2008) 016005 [hep-ph/0611312] [SPIRES].
- [23] J. Bagger, E. Poppitz and L. Randall, *The R axion from dynamical supersymmetry breaking*, *Nucl. Phys. B* **426** (1994) 3 [hep-ph/9405345] [SPIRES].
- [24] K. Griest and D. Seckel, *Three exceptions in the calculation of relic abundances*, *Phys. Rev. D* **43** (1991) 3191 [SPIRES].
- [25] P. Gondolo and G. Gelmini, *Cosmic abundances of stable particles: improved analysis*, *Nucl. Phys. B* **360** (1991) 145 [SPIRES].
- [26] H.-S. Goh and M. Ibe, *R-axion detection at LHC*, *JHEP* **03** (2009) 049 [arXiv:0810.5773] [SPIRES].
- [27] T. Moroi, H. Murayama and M. Yamaguchi, *Cosmological constraints on the light stable gravitino*, *Phys. Lett. B* **303** (1993) 289 [SPIRES].
- [28] M. Viel, J. Lesgourgues, M.G. Haehnelt, S. Matarrese and A. Riotto, *Constraining warm dark matter candidates including sterile neutrinos and light gravitinos with WMAP and the Lyman- α forest*, *Phys. Rev. D* **71** (2005) 063534 [astro-ph/0501562] [SPIRES].
- [29] M. Ibe, K.I. Izawa, Y. Nakayama, Y. Shinbara and T. Yanagida, *Conformally sequestered SUSY breaking in vector-like gauge theories*, *Phys. Rev. D* **73** (2006) 015004 [hep-ph/0506023] [SPIRES].
- [30] CHARM collaboration, F. Bergsma et al., *Search for axion like particle production in 400-GeV proton-copper interactions*, *Phys. Lett. B* **157** (1985) 458 [SPIRES].
- [31] CLEO collaboration, W. Love et al., *Search for very light CP-odd Higgs boson in radiative decays of $\Upsilon(1S)$* , *Phys. Rev. Lett.* **101** (2008) 151802 [arXiv:0807.1427] [SPIRES].
- [32] Z. Chacko, M.A. Luty and E. Ponton, *Calculable dynamical supersymmetry breaking on deformed moduli spaces*, *JHEP* **12** (1998) 016 [hep-th/9810253] [SPIRES].
- [33] M. Ibe and R. Kitano, *Gauge mediation in supergravity and gravitino dark matter*, *Phys. Rev. D* **75** (2007) 055003 [hep-ph/0611111] [SPIRES].